Nanoscale

Accepted Manuscript

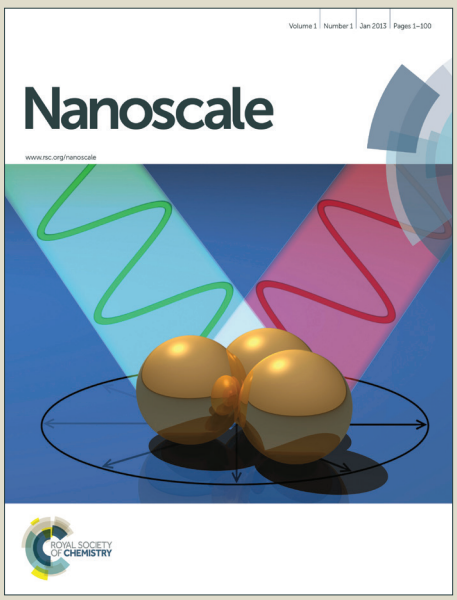

ROYAL SOCIETY OF CHEMISTRY

www.rsc.org/nanoscale

Cite this: DOI: 10.1039/c0xx00000x

www.rsc.org/xxxxxx

ARTICLE TYPE

Halide Ion-Mediated Growth of Single Crystalline Fe Nanoparticles

Sen Zhang,[†,§] Guangming Jiang,[‡,§] Gabriel T. Filsinger,[†] Liheng Wu,[†] Huiyuan Zhu,[†] Jonghun Lee,[†] Zhongbiao Wu,[‡] Shouheng Sun[†,*]

Received (in XXX, XXX) Xth XXXXXXXXX 20XX, Accepted Xth XXXXXXXXX 20XX
DOI: 10.1039/b000000x

We report a facile halide ion (Cl^- or Br^-) mediated synthesis of Fe nanoparticles (NPs) by thermal decomposition of $Fe(CO)_5$. The NP structure is controlled to be either amorphous (in the absence of halide ions) or single crystalline *bcc* (in the presence of halide ions). Through systematic investigation on the synthetic conditions, we have confirmed that the formation of *bcc*-Fe NPs is facilitated by the strong interactions between halide ions and Fe, which favors thermodynamic growth of Fe over the existing Fe NPs. Compared with the amorphous Fe NPs, the *bcc*-Fe NPs exhibit much enhanced magnetization values and chemical stability. This halide ion mediated growth may become a general strategy to control the growth of metallic NPs, especially first-row transition metal NPs, in a thermodynamically more stable way, producing single crystalline NPs with much controlled physical and chemical properties for magnetic and catalytic applications.

Introduction

Rational tuning of nanoparticles (NPs) is essential in developing functional NPs for nanotechnological applications.[1-5] Recent efforts have led to the formation of various NPs with well-defined sizes, shapes, compositions and structures.[6-10] Among the parameters studied, NP's crystalline structure is an important one because the atomic arrangements in metallic NPs can dramatically influence NP properties in catalysis, magnetism and optics.[11-15] In the bulk form, the metal's structure, ranging from amorphous to various crystalline phases, can be readily controlled by thermal treatment. But it is often difficult to apply this thermal treatment directly to NPs, especially the first-row transition metal NPs, as they tend to aggregate and/or sinter under high temperature thermal annealing conditions.[16-18] Since solution phase reaction has been applied more often to prepare monodisperse NPs, it is highly desirable to control crystal structure within each NP when it is formed in the reaction condition.

Here we report an improved synthesis of monodisperse body centered cubic Fe (*bcc*-Fe) NPs in the presence of halide ions. Bulk Fe is strongly ferromagnetic with high magnetic moment and large susceptibility. Fe NPs in the diameter smaller than 20 nm are often superparamagnetic and can serve as promising probes for magnetic resonance imaging, drug delivery and magnetic detection.[19-25] Monodisperse amorphous Fe (amor-Fe) NPs are commonly prepared by pyrolysis of iron pentacarbonyl, $Fe(CO)_5$.[26-32] Crystallized *bcc*-Fe NPs are also synthesized similarly but in the presence of hexadecylammonium chloride (HDA·HCl) or cetyltrimethylammonium bromide (CTAB).[33, 34] This HDA·HCl or CTAB induced formation of *bcc*-Fe led us to explore further the co-surfactant effect on controlling Fe NP growth and crystallization in the condition that is otherwise the same as in the synthesis of amor-Fe NPs *via* $Fe(CO)_5$ decomposition. We focused on the anion effect on NP formation by adding different small molecular salts and found that the halide ions (Cl^-, Br^-) played an important role in Fe-growth into *bcc*-Fe NPs during the synthesis. Our synthetic study indicated that the strong binding of Cl^- or Br^- and Fe induced a slow Fe growth kinetics, facilitating the addition of Fe atoms in a thermodynamically more stable way and the formation of Fe NPs with better crystallinity. This halide ion effect may be generalized to control the growth of metallic NPs, especially the first-row transition metal NPs, into desired crystal structures.

Materials and Methods

Materials

Iron pentacarbonyl ($Fe(CO)_5$), oleylamine (70%), oleic acid (90%), 1-octadecene (ODE, 90%), 1,2,3,4-tetrahydronaphthalene (Tetralin, ≥97%), ammonium chloride (NH_4Cl, ≥99%), ammonium bromide (NH_4Br, 99.9%), or iron chloride ($FeCl_2$, 98%), or ammonium sulfide ($(NH_4)_2SO_4$, ≥99%), trimethylamine N-oxide ($(CH_3)_3NO$, 98%), hexanes, hexadecylamine (HDA, 90%) and hydrogen chloride solution (HCl, 1 M in diethyl ether) were purchased from Sigma Aldrich and used without any further purification. Hexadecylammonium chloride (HDA.HCl) was synthesized following a published work.[33] In detail, 12 mL of HCl solution was added slowly into the a solution of HDA (10 mmol, 2.4 g) in 150 mL of hexane with the ice-bath cooling. The mixture was stirred at room temperature for 2 hours and centrifuged (5000 rpm, 5 min) to collect the white precipitate of

HDA.HCl. The HDA.HCl was washed for 3 times with hexane and dried in ambient condition for further usage.

Synthesis of *bcc*-Fe NPs

Under a gentle flow of N_2, 54 mg of NH_4Cl (1 mmol) was mixed and magnetically stirred with 20 mL of tetralin and 1 mL of oleylamine, OAm. The mixture was heated to 120 ºC and kept at this temperature for 30 min to generate a colorless solution. Under a blanket of N_2, the solution was heated to 180 ºC and 0.7 mL of iron pentacarbonyl ($Fe(CO)_5$, 5.4 mmol) was injected into the solution. The color of the solution changed to yellow-brown-dark brown-black in 8 min. The solution was kept at 180 ºC for 30 min before it was cooled to room temperature. The NPs were separated by adding isopropanol (50 mL), followed by centrifugation (8500 rpm, 8 min). The NPs were further purified by dispersing into hexane (20 mL) and adding ethanol (50 mL) and centrifugation (8500 rpm, 8 min). The as-synthesized 12.5 nm Fe NPs were dispersed in hexane.

In the same reaction condition, 0.3 mL $Fe(CO)_5$ gave 10 nm Fe NPs and 1.4 mL $Fe(CO)_5$ yielded 17 nm Fe NPs. Similarly, the reaction was also run in the presence of 1 mmol NH_4Br, or 0.5 mmol $FeCl_2$, or 0.5 mmol $(NH_4)_2SO_4$, or 1 mmol HDA.HCl instead of NH_4Cl, respectively, to study the cation and anion effects.

Synthesis of amor-Fe NPs

Amorphous Fe NPs were prepared by decomposition of $Fe(CO)_5$ without any halide additives. Typically, 0.7 mL $Fe(CO)_5$ reacting in a solution of 20 mL of tetralin and 1 ml of OAm at 180 ºC and at N_2 blanket can yield 13 nm amor-Fe NPs. The amor-Fe NPs were purified through the same procedures as described above in the synthesis of *bcc*-Fe NPs.

Solution-phase oxidation of Fe NPs

30 mg of $(CH_3)_3NO$ was stirred with 20 mL of ODE and heated to 130 ºC under a N_2 flow for 1 h to remove the moistures. A dispersion of 80 mg of as-synthesized Fe NPs (*bcc*-Fe and amor-Fe) in hexane was added to the mixture. The reactants were kept at 130 ºC for 1 h to remove hexane and then heated at 210 ºC for 2 hrs before cooling to room temperature. The NPs were purified through the same procedures as described above in the synthesis of *bcc*-Fe NPs.

NPs Characterization

X-ray diffraction (XRD) characterizations were carried out on a Bruker AXS D8-Advanced diffractometer with Cu Kα radiation (λ =1.5418 Å). Samples for transmission electron microscopy (TEM) analysis were prepared by depositing a drop of diluted NP dispersion in hexane on amorphous carbon coated copper grids. TEM images were obtained using a Philips CM 20 (200 kV). High resolution TEM (HRTEM) images were obtained using a JEOL 2100 (200 kV). The magnetic properties of the NPs were measured by Vibrating Sample Magnetometer (VSM) (LakeShore, 7404) with a field up to 1.5 kOe. To obtain NP powder for magnetic measurement, the NPs were precipitated from their hexane dispersion by ethanol, washed with ethanol, and dried at room temperature. Each sample was loaded into a gelatin capsule (0.3 ml, Electron Microscopy Science) and fixed in position with a cotton ball.

Results and Discussion

Synthesis of *bcc*-Fe and amor-Fe NPs

Amor-Fe and *bcc*-Fe NPs were both synthesized via thermal decomposition of $Fe(CO)_5$ in tetralin at 180 ºC and the resultant Fe NPs were stabilized by OAm. Similar to what was reported in $Fe(CO)_5$ pyrolysis in ODE,[32] our current synthesis yielded 13 nm ± 0.5 nm amor-Fe NPs (**Figure 1A**). But when HDA.HCl was added in the reaction mixture, 12.5 nm ± 0.5 nm *bcc*-Fe NPs were obtained (**Figure 1B**). To investigate what dominates the formation of *bcc*-Fe over amor-Fe, we replaced the HDA.HCl with ammonium chloride, NH_4Cl, in the synthesis and found that the *bcc*-Fe NPs were still formed. TEM image show that the Fe NPs prepared with NH_4Cl also have an average size of 12.5 nm ± 0.5 nm (**Figure 1C**). XRD patterns of the Fe NPs prepared with and without the presence of NH_4Cl as well as those in the presence of HDA.HCl (**Figure 2**) show the characteristic *bcc*-Fe peaks. Comparing with **Figure 1B**, **C** and **2**, we can see that the cationic units in NH_4Cl and HDA.HCl have no effect on NP growth. The presence of Cl^- is a dominant factor for the formation of *bcc*-Fe NPs. The HRTEM image of a representative Fe NP further demonstrated that the 12.5 nm Fe NP has a 8.5 nm core of single crystalline Fe with the typical *bcc*-Fe lattice fringe (0.20 nm of (100) plane), and a 2.0 nm shell of polycrystalline Fe_3O_4 (0.24 nm spacing of (222) plane) generated by the surface oxidation (**Figure 1D**).

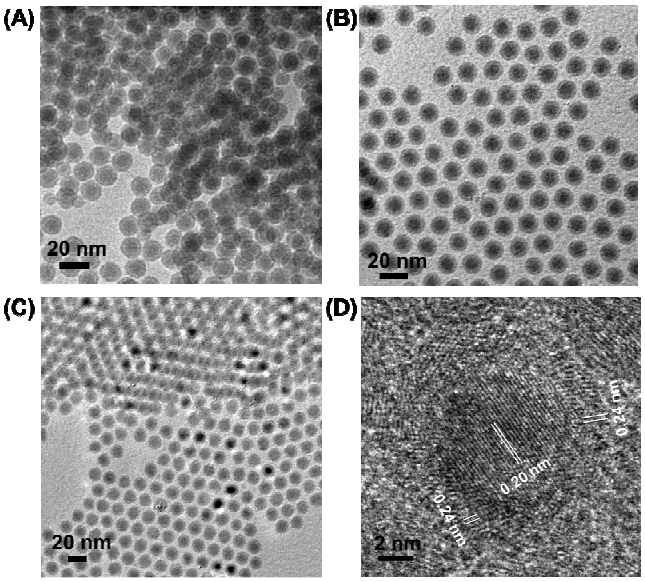

Figure 1. (A-C) TEM images of the as-synthesized (A) 13 nm amor-Fe NPs, (B) 12.5 nm *bcc*-Fe NPs obtained in the presence of HDA.HCl and (C) 12.5 nm *bcc*-Fe NPs obtained in the presence of NH_4Cl. (D) HRTEM image of a representative single crystalline *bcc*-Fe NP. The single crystalline *bcc*-Fe NPs were synthesized in the presence of NH_4Cl.

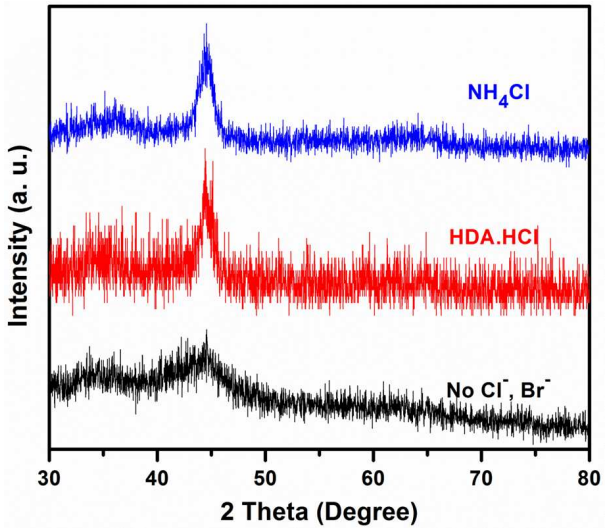

Figure 2. XRD patterns of the as-synthesized Fe NPs made without and with halide ions.

We also tested the effect of NH_4Br on the growth of Fe NPs and found that the Fe NPs separated from the synthesis were nearly the same with those obtained in the presence of NH_4Cl. (**ESI**†, **Figure S1A**). To further confirm that halide effect is dominant on Fe NP growth, we synthesized Fe NPs in the same condition by replacing NH_4Cl with iron chloride, $FeCl_2$, or ammonium sulfate, $(NH_4)_2SO_4$. When $FeCl_2$ was present, monodisperse 11 nm *bcc*-Fe NPs were separated (**ESI**†, **Figure S1B and Figure S2**). However, in the presence of $(NH_4)_2SO_4$ polydisperse amor-Fe NPs were obtained (**ESI**†, **Figure S1C and Figure S3)**. Our studies indicated clearly that halide ions (Cl^-, Br^-) were crucial for generating monodisperse single crystalline *bcc*-Fe NPs.

Formation mechanism of halide-ion induced *bcc*-Fe NPs

We monitored the Fe NP growth in the reaction to demonstrate the role Cl^- played in the synthesis. **Figure 3** shows the morphology evolutions of both amor-Fe and *bcc*-Fe NPs by separating NPs from the reaction systems at different reaction times. Without Cl^-, the solution turned to "black" within 10 seconds after the injection of $Fe(CO)_5$, suggesting fast Fe nucleation. Fe NPs separated from the reaction mixture 3, 6 and 20 min after $Fe(CO)_5$ injection did not show much size difference (**Figure 3A-C**), indicating that the amor-Fe NPs were formed quickly (less than 5 min) after the $Fe(CO)_5$ injection. In contrast, when Cl^- was present, the reaction solution slowly became yellow, brown, dark-brown, and then turned to black in 8 min. The NPs separated at 10 min were only about 5 nm, and then grew to 10 nm and 12.5 nm at 20 and 30 min, respectively (**Figure 3D-F**). These results show that Cl^- can efficiently inhibit the Fe growth kinetics, facilitating the formation of *bcc*-Fe NPs. Previously, halide ions were demonstrated to tune the shape of the Pd based NPs due to the binding difference of halide ions on different crystalline facets.[35-37] In our example, the Cl^-, (or Br^-) ion does not show crystal-facet dependent growth. As illustrated in **Figure 4**, we hypothesize that strong binding between Fe-Cl slows-down the growth of Fe on the seeding NP surface, favoring thermodynamic growth of the NPs into the *bcc* structure.

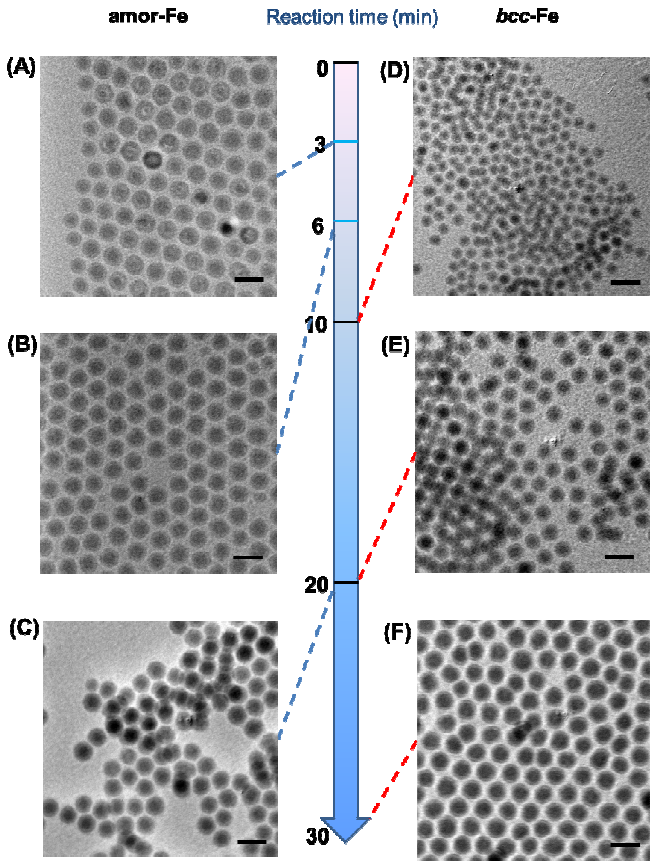

Figure 3. TEM images of the amor-Fe NPs separated 3 (A), 6 (B) and 20 min (C) after injecting the $Fe(CO)_5$, and the single crystalline Fe NPs obtained 10 (D), 20 (E) and 30 min (F) after injecting the $Fe(CO)_5$. The single crystalline Fe NPs were synthesized in the presence of NH_4Cl. The inset scale bar is 20 nm.

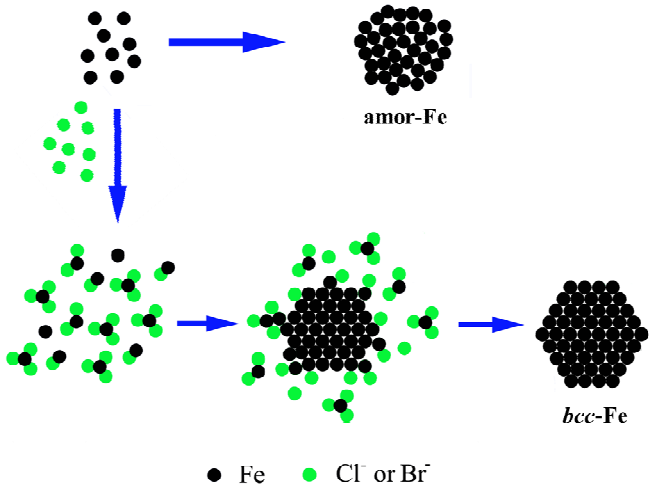

Figure 4. Schematic illustration of formation of single crystalline *bcc*-Fe NPs in the presence of halide ions.

Size control of the *bcc*-Fe NPs

The sizes of the *bcc*-Fe NPs could be tuned by controlling the $Fe(CO)_5$ amount. As summarized in **Tab. S1** (**ESI**[†]), when 0.3 mL $Fe(CO)_5$ and 1.4 ml $Fe(CO)_5$ were used, 10 nm and 17 nm Fe NPs were produced respectively (**Figure 5**). This is because the increase in precursor concentration can provide more Fe atoms for NPs to grow, which was also observed in some oxide NPs systheses.[38, 39] The amount of OAm present in the reaction solution also affected Fe NP formation. For example, in the condition used to make 17 nm Fe NPs, when excess amount of OAm (3 mL instead of 1 mL) was used, 13 nm Fe NPs were separated. It looks that the increase of OAm in the reaction mixture raises the Fe nucleation threshold, leading to more consumption of Fe for the formation of Fe nuclei and yielding smaller Fe NPs.

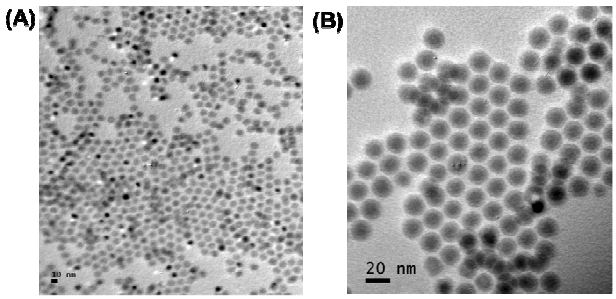

Figure 5. TEM images of the Fe NPs obtained from (A) 0.4 ml $Fe(CO)_5$ and (B) 1.4 ml $Fe(CO)_5$ in the presence of NH_4Cl.

Enhanced chemical and magnetic stability of *bcc*-Fe NPs

Magnetic properties of the Fe NPs (in dry powder form precipitated from hexane solution) were analyzed by VSM. As shown in **Fig. 6A**, the as-synthesized 12.5 nm *bcc*-Fe NPs obtained in the presence of NH_4Cl are superparamagnetic at room temperature and have a saturation magnetization value (M_s) of 84.8 emu/g_{NPs}, much higher than the amor-Fe NPs (M_s = 65.1 emu/g_{NPs}). After subtracting the organic stabilizer, the M_s of the *bcc*-Fe and the amor-Fe NPs reached 121 emu/g_{Fe} and 95.5 emu/g_{Fe} respectively, lower than the bulk vale at 220 emu/g_{Fe}. This magnetic moment reduction is caused by surface oxidation of the Fe NPs.

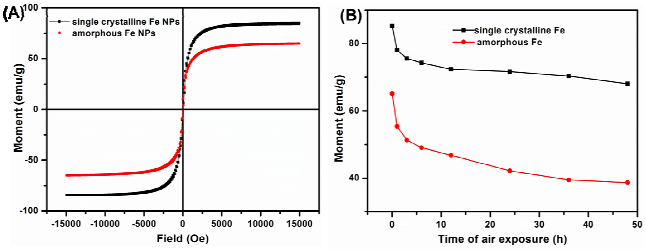

Figure 6. (**A**) The hysteresis loops of the 12.5 nm *bcc*-Fe NPs and amor-Fe NPs at room temperature. (**B**) The change of saturation magnetization values of the 12.5 nm *bcc*-Fe and the amor-Fe NPs as a function of air exposure time at room temperature.

More oxidation studies indicated that the *bcc*-Fe NPs showed much enhanced chemical and magnetic stability than the amor-Fe NPs (**Figure 6B**). After exposure to air, the 12.5 nm *bcc*-Fe NPs lost some values in magnetic moment due to surface oxidation in the first 6 h exposure to air, and then reached a stable plateau after 2 days with their M_s stabilized at 68.1 emu/g_{NPs}, a 19.7% magnetic moment loss. In contrast, 13 nm amor-Fe NPs had a faster magnetic moment loss initially, and a continued drop to 38.6 emu/g_{NPs} (a 40.7% loss) after 2 days. This stability enhancement in *bcc*-Fe NPs is attributed to the formation and stabilization of the crystalline Fe_3O_4 shell around Fe core.

This chemical stability increase demonstrated in the *bcc*-Fe NPs was even more apparent in the solution oxidative conditions. By reacting the Fe NPs with oxygen transferring agent trimethylamine N-oxide, $(CH_3)_3NO$, at high temperature (210 °C) in ODE solvent[40], the amor-Fe NPs were fully oxidized to hollow Fe_3O_4 NPs through Kirkendall effect[41-45], while in the same reaction/oxidation condition, the *bcc*-NPs still preserved some Fe cores in a form of york-shell Fe-Fe_3O_4 structure (**Figure 7**).

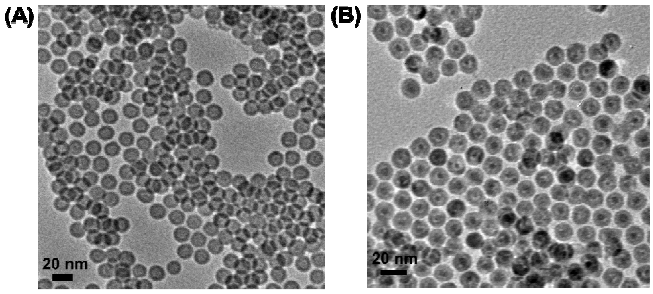

Figure 7. TEM images of (**A**) amor-Fe NPs and (**B**) *bcc*-Fe NPs after reacting with $(CH_3)_3NO$ at 210 ºC for 2 h.

Conclusions

We have reported a halide ion (Cl^- or Br^-) mediated synthesis of Fe NPs, with NP structure controlled to be either amorphous (in the absence of halide ions) or single crystalline *bcc* (in the presence of halide ions), through the facile thermal decomposition of $Fe(CO)_5$. Our systematic investigation on the synthetic conditions and NP growth mechanism confirmed that the formation of *bcc*-Fe NPs is facilitated by the strong interactions between halide ions and Fe, which favors thermodynamic growth of Fe over the existing Fe nuclei and seeds. Compared with the amorphous Fe NPs, the *bcc*-Fe NPs exhibit much enhanced magnetization values and chemical and magnetic stabilities. This halide ion mediated growth may become a general strategy to control the growth of metallic NPs, especially first-row transition metal NPs, in a thermodynamically more stable way, producing crystalline structure tunable NPs with much controlled physical and chemical properties for magnetic and catalytic applications.

Acknowledgments

Supported in part by the INSIC (Information Storage Industry Consortium). G.J. thanks the support from China Scholarship Council.

Notes and references

† *Department of Chemistry, Brown University, Providence, Rhode Island 02912, USA; Fax: 401-863-9046; Tel: 401-863-3329; E-mail: ssun@brown.edu*

‡ *Department of Environmental Engineering, Zhejiang University, Hangzhou, Zhejiang 310058, China.*

§ *These authors contributed equally to this work.*

† Electronic Supplementary Information (ESI) available: Table S1, Figure S1-3. See DOI: 10.1039/b000000x/

1. D. V. Talapin, J. –S. Lee, M. V. Kovalenko and E. V. Shevchenko, *Chem. Rev.* **2010**, *110*, 389-458.
2. C. B. Murray, C. R. Kagan and M. G. Bawendi, *Annu. Rev. Mater. Sci.* **2000**, *30*, 545-610.
3. Y. –W. Jun, J. –W. Seo and J. Cheon, *Acc. Chem. Res.* **2008**, *41*, 179-189.
4. S. Guo, S. Zhang and S. Sun, *Angew. Chem. Int. Ed.* **2013**, *52*, 8526-8544.
5. P. D. Cozzoli, T. Pellegrino and L. Manna, *Chem. Soc. Rev.* **2006**, *35*, 1195-1208.
6. J. Lee, S. Zhang and S. Sun, *Chem. Mater*. **2013**, *25*, 1293-1304.
7. J. Park, J. Joo, S. G. Kwon and T. Hyeon, *Angew. Chem. Int. Ed.* **2007**, *46*, 4630-4660.
8. S. Zhang, J. Lee and S. Sun, *Open. Surf. Sci. J.* **2012**, *4*, 26-34.
9. X. Liu, D. Wang and Y. Li, *Nano Today* **2012**, *7*, 448-466.
10. S. Guo, S. Zhang, S. Dong and S. Sun, *J. Am. Chem. Soc.* **2013**, *135*, 13879-13884.
11. S. Sun, C. B. Murray, D. Weller, L. Folks and A. Moser, *Science* **2000**, *287*, 1989-1992.
12. S. Sun and C. B. Murray, *J. Appl. Phys.* **1999**, *85*, 4325-4330.
13. X. Ye, J. E. Collions, Y. Kang, J. Chen, D. T. N. Chen, A. G. Yohn and C. B. Murray, *Proc. Natl. Acad. Sci. USA* **2010**, *107*, 22430-22435.
14. S. Zhang, S. Guo, H. Zhu, D. Su and S. Sun, *J. Am. Chem. Soc.* **2012**, *134*, 5060-5063.
15. D. Wang, H. L. Xin, R. Hovden, H. Wang, Y. Yu, D. A. Muller, F. J. DiSalvo and H. D. Abruna, *Nat. Mater.* **2012**, *12*, 81-87.
16. Z. R. Dai, S. Sun and Z. L. Wang, *Nano Letters*. **2001**, *1*, 443-447.
17. H. Chen, D. Wang, Y. Yu, K. A. Newton, D. A. Muller, H. D. Abruña and F. J. DiSalvo, *J. Am. Chem. Soc.* **2012**, *134*, 18453-18459.
18. H. Zeng, J, Li, J. P. Liu, Z. L. Wang and S. Sun, *Nature* **2002**, *420*, 395-398.
19. D. L. Huber, *Small* **2005**, *1*, 482-501.
20. F. Dumestre, B. Chaudret, C. Amiens, P. Renaud and P. Fejes, *Science* **2004**, *303*, 821-823.
21. T. J. Yoon, H. Lee, H. Shao and R. Weissleder, *Angew. Chem. Int. Ed.* **2011**, *50*, 4663-4666.
22. H. Lee, T. J. Yoon and R. Weissleder, *Angew. Chem. Int. Ed.* **2009**, *48*, 5657-5660.
23. L. –M. Lacroix, S. Lachaize, A. Falqui, M. Respaud and B. Chaudret, *J. Am. Chem. Soc.* **2009**, *131*, 549-557.
24. N. Lee and T. Hyeon, *Chem. Soc. Rev.* **2012**, *41*, 2575-2589.
25. H. Don, X. Sun and S. Sun, *Acc. Chem. Res.* **2011**, *44*, 875-882.
26. C. H. Griffiths, M. P. O'Horo and T. W. Smith, *J. App. Phys*, **1979**, *50*, 7108-7115.
27. J. V. Wonterghem, S. Mørup, S. W. Charles, S. Wells, J. Villadsen, *Phys. Rev. Lett,* **1985**, *55*, 410-413.
28. W. Pei, S. Kakibe, I. Ohta and M. Takahashi, *IEEE Trans. Magn.* **2005**, *41*, 3391-3393.
29. H. Shao, H. Lee, Y. Huang, I. Ko and C. Kim, *IEEE Trans. Magn.* **2005**, *41*, 3388-3390.
30. S. –J. Park, S. Kim, S. Lee, Z. G. Khim, K. Char and T. Hyeon, *J. Am. Chem. Soc.* **2000**, *122*, 8581-8582.
31. D. Farrell, S. A. Majetich and J. P. Wilcoxon, *J. Phys. Chem. B* **2003**, *107*, 11022-11030.
32. S. Peng, C. Wang, J. Xie and S. Sun, *J. Am. Chem. Soc.* **2006**, *128*, 10676-10677.
33. L. M. Lacroix, D. Ho, N. F. Hulls, X. Sun, K. Chen and S. Sun, *Nano Lett*. **2011**, *11*, 1641-1645.
34. C. Yang, H. Zhao, Y. Hou and D. Ma, *J. Am. Chem. Soc.* **2012**, *134*, 15814-15821.
35. Y. Xia, Y. Xiong, B. Lim and S. E. Skrabalak, *Angew. Chem. Int. Ed.* **2008**, *48*, 60-103.
36. T. Yu, D. Y. Kim, H. Zhang and Y. Xia, *Angew. Chem. Int. Ed.* **2011**, *50*, 2773-2777.
37. X. Xia, S. Xie, M. Liu, H. –C. Peng, N, Lu, J. Wang, M. J. Kim and Y. Xia, *Proc. Natl. Acad. Sci. USA* **2013**, *110*, 6669-6673.
38. D. Kim, N. Lee, M. Park, B. H. Kim, K. An and T. Hyeon, *J. Am. Chem. Soc.* **2009**, *131*, 454-455.
39. H. Zeng, P. M. Rice, S. X. Wang and S. Sun, *J. Am. Chem. Soc.* **2004**, *126*, 11458-11459.
40. S. Peng and S. Sun, *Angew. Chem. Int. Ed.* **2007**, *46*, 4155-4158.
41. Y. Yin, R. M. Rioux, C. K. Erdonmez, S. Hughes, G. A. Somorjai and A. P. Alivisatos, *Science* **2004**, *304*, 711 – 714.
42. Y. Yin, C. K. Erdonmez, A. Cabot, S. Hughes and A. P. Alivisatos, *Adv. Funct. Mater.* **2006**, *16*, 1389 – 1399.
43. R.-K. Chiang and R.-T. Chiang, *Inorg. Chem.* **2007**, *46*, 369-371.
44. A. E. Henkes, Y. Vasquez and R. E. Schaak, *J. Am. Chem. Soc.* **2007**, *129*, 1896-1897.
45. J. Gao, G. Liang, B. Zhang, Y. Kuang, X. Zhang and B. Xu, *J. Am. Chem. Soc.* **2007**, *129*, 1428-1433.

TOC